Articles in PresS. Am J Physiol Endocrinol Metab (January 28, 2004). 10.1152/ajpendo.00427.2003

E-00427-2003.R1

FINAL ACCEPTED VERSION

THE CATABOLIC ACTION OF INSULIN IN RAT ARCUATE NUCLEUS IS NOT ENHANCED BY EXOGENOUS 'TUB' EXPRESSION

Dianne P. Figlewicz [1,2], Aryana Zavosh[2], Timothy Sexton [3], and John F. Neumaier[3]

[1]Metabolism/Endocrinology (151), VA Puget Sound Health Care System, 1660 So. Columbian Way, Seattle, Washington 98108 U.S.A.
[2] Dept of Psychiatry and Behavioral Sciences, University of Washington, Seattle, Washington 98195-6560 U.S.A.
[3]Dept. of Psychiatry and Behavioral Sciences, University of Washington, Harborview Medical Center, 325 9th Ave., Seattle, Washington 98104 U.S.A.

Correspondence should be addressed to:
Dianne Figlewicz Lattemann, Ph.D.
VA Puget Sound Health Care System (151)
1660 So. Columbian Way
Seattle WA 98108 U.S.A.
(latte@u.washington.edu)
Phone: 206-768-5240
FAX: 206-764-2164

Running title: CNS insulin and 'tub' in the rat

ABSTRACT

The central nervous system (CNS) protein ‘tub’ has been identified from the genetically obese ‘tubby’ mouse. While the native function of ‘tub’ *in situ* is not understood, cell-based studies suggest that one of its roles may be as an intracellular signaling target for insulin. In normal animals, insulin acts at the hypothalamic arcuate nucleus to regulate energy balance. Here we used a Herpes Simplex viral expression system to evaluate whether ‘tub’ overexpression in the arcuate nucleus (ARC) of normal rats enhances this action of insulin. In chow-fed rats, ‘tub’ overexpression had no effect on insulin action. In rats fed a high fat diet snack in addition to chow, simulating the diet of Westernized societies, the body weight regulatory action of insulin was impaired, and ‘tub’ overexpression further impaired insulin action. Thus, an excess of ‘tub’ at the arcuate nucleus does not enhance the *in vivo* effectiveness of insulin, and is not able to compensate for the ‘downstream’ consequences of a high fat diet to impair CNS body weight regulatory mechanisms.

Key Words: food intake body weight hypothalamus

Over the past two decades, intense investigation from a number of laboratories has focused on the identification of critical peptides and proteins that act in brain pathways to regulate food intake, body weight, and energy balance (1,27). One such protein that is implicated in the CNS regulation of energy balance is *tub*. The 'tubby' mouse was described by Coleman and Eicher in 1990 (9) as a spontaneously occurring, autosomal recessive mutant characterized by adult-onset obesity and insulin resistance. The *tub* protein has been cloned, as have other members of this unique family of proteins (13,16,18,20,21), and it is now known that a C-terminal mutation of this protein is responsible for the 'tubby' mouse phenotype. Kapeller and colleagues replicated this phenotype by creating a targeted deletion of the *tub* mouse gene: Knockout of the *tub* gene in normal mice recapitulates the 'tubby' phenotype and demonstrates that the naturally occurring mutation is a loss-of-function mutation (28). *Tub* protein is expressed in the central nervous system (CNS) in neurons (14,24) and has been localized in several hypothalamic nuclei which express insulin receptors and are implicated in the control of body weight, metabolism, and energy balance (3). Consistent with a CNS role for '*tub*' in body weight regulation, mRNA levels for ARC POMC (the precursor of the anorectic α-MSH) are decreased and mRNA levels for the orexigenic peptide NPY in the DMH/VMH are increased in mature 'tubby' mice (12). The human homologue of *tub* has been mapped (7) but the relevance of *tub* to human obesity requires further study: one report to date has examined a group of 105 morbidly obese Finnish patients and reported no significant linkage in these subjects between obesity and the human *tub* gene (23). This is perhaps not surprising considering that the complete knockout of the *tub* gene results in a less severe, adult-onset obesity. Because retinal degeneration secondary to

apoptosis is also observed in ‘tubby’ mice, it was suggested that localized hypothalamic apoptosis (comparable to a ‘genetic VMH lesion’) might account for the obesity. However, apoptotic markers have not been found in the ‘tubby’ hypothalamus.

To date, there have been few studies evaluating the cellular functions of *tub*. One line of study suggests that *tub* may function in the CNS as a critical molecule in the downstream insulin receptor signaling path. Kapeller *et al*. have demonstrated in intact cells and in *in vitro* kinase systems that *tub* is tyrosine-phosphorylated by the activated insulin receptor kinase (as well as by Abl and JAK 2, but not EGFR or Src kinases) (15). In the phosphorylated state, *tub* associates with the SH2 domains of a number of cell signaling molecules including the C-terminal SH2 domain of PLCγ (15). These findings were interpreted to suggest that *tub* can be a substrate in the pathway of intracellular insulin action, and may function as an adaptor, linking insulin to intracellular signaling cascades. Boggon and colleagues used functional genomics to further characterize the cellular actions of *tub* (4). Their studies suggest that the C-terminal, highly conserved portion of the protein is a DNA-binding structure, and the N-terminal portion may be a regulator of transcription. This is supported by the observation that *tub* was highly localized to the nucleus of neurons in primary culture. *Tub* has also been shown to translocate from the plasma membrane to the nucleus following serotonin activation of 5-HT2c receptors (4); this may bear on control of food intake since 5-HT2c knockout mice develop mild, adult-onset obesity and insulin resistance (29). Thus, *tub* may serve as a transcription factor as well as an ‘adaptor’ molecule.

We and others have demonstrated that the pancreatic hormone insulin (3,11,27) can act in the CNS as an adiposity signal. A particular hypothalamic target for this action is the ARC, where coordinate increased expression of anorexic, and decreased expression of orexigenic, peptides has been reported (3,22,27,30). One component mechanism underlying the obesity of the 'tubby' phenotype might be an impairment of insulin intracellular signaling in the ARC. In the present study, in order to further evaluate *tub* function in normal non-obese animals, we asked whether increased expression of *tub* above normal endogenous levels can enhance behavioral sensitivity to endogenous insulin or to exogenous, locally administered insulin in the rat. The ability of exogenous insulin to decrease body weight is impaired in rats fed a high fat diet, either independent of, or accompanied by, dietary obesity (2,6). Thus, with access to a high fat diet and development of dietary obesity--a model of the mild to moderate obesity that is prevalent in "Westernized" societies--insulin resistance occurs in the CNS as well as in peripheral target tissues. We hypothesized that if *tub* functions as an adaptor for intracellular insulin signaling, then in a model of CNS insulin resistance (high fat feeding), the catabolic action of exogenously administered insulin would be impaired but this might be corrected or reversed by increasing *tub* expression. Using a Herpes simplex viral vector system, we targeted the ARC of the hypothalamus as a location of neurons that synthesize insulin receptors, and as a CNS site that is sensitive to insulin effects on energy balance.

MATERIALS AND METHODS

Assurances. All procedures performed in these studies were approved by the VA Puget Sound Health Care System and University of Washington committees for humane use of animals (rat studies) and Biohazard/Biosafety (preparation and use of Herpes simplex engineered viral vectors).

Materials. Unless otherwise indicated, reagents were obtained from Sigma (St. Louis MO). Insulin for ARC infusions was Novolin (Novo Nordisk, 100 U/ml) diluted with sterile synthetic cerebrospinal fluid (CSF) solution.

Preparation of HA-*tub*-GFP viral particles. Modification of our previously published methodology for the preparation of HSV-vector particles was utilized to prepare HA-*tub* expressing viral particles (8). This vector/amplicon system has been characterized to target neurons,with low toxicity and good efficiency of gene expression (see discussion in [8]). The clone for rat *tub* was provided by Dr. Rosana Kapeller, Millenium Pharmaceuticals. As there are no available antibodies for rat 'tub', and available antibodies directed at mouse 'tub' do not detect endogenous 'tub' in rat CNS (Figlewicz Lattemann and Baskin, unpublished observations), a hemagglutinin (HA) tag was introduced into the rat 'tub' construct. The HA tag does not interfere with insulin-stimulated phosphorylation (or other biochemical actions) of the 'tub' protein (16). For ease of visualization within the CNS, the vector system also expressed green fluorescent protein (GFP; see below for validation of the co-expression of these proteins), a standard approach for rapid visualization of successful infection or transfection. In order to

introduce the HA epitope tag into the N-terminus of the rat *tub* gene, pN10-r*Tub* was used as a template to PCR clone the rat *tub* full length sequence using a downstream primer (5' AGATCTAGACTACTCGCAGGCCAGCT 3') and an upstream primer (5' AGATCTAGACCCATGGGGTACCCATATGACGTCCCAGACTACGCCACTTCCA AGCCGCATT 3') that introduced an in-frame HA epitope. To enable further manipulation the resulting product was used as a PCR template with an upstream primer (5' GCGCGGATCCTGGCGGCCGCTCTA 3') containing a BamH I and a Not I site and the downstream primer (5' GCGCGCTAGCAGCCCGGGGGATCC 3') containing a BamH I, Sma I and an Nhe I site. An HSV amplicon expressing both HA-*tub* and GFP was then constructed by cutting the second PCR product with BamH I and ligating it into the BamH I/Avr II cut multiple cloning site of the previously constructed p1003 amplicon (8). The p1003 amplicon contains two separate transcriptional units. The first transcriptional unit consists of the HSV IE 4/5 promoter followed by a multiple cloning site and a SV40 polyA signal. The second transcriptional unit consists of the CMV promoter followed by the eGFP gene and a SV40 polyA signal (8). DNA sequencing confirmed the identity and directionality of the HA-*tub* insert in the resulting amplicon (HA-*tub*/GFP) which was further studied using standard transfection techniques, or packaged into non-replicating HSV virion particles as previously described (19) to produce the viral vector. The construct was sequenced in its entirety to verify complete and accurate identity of the tub open reading frame, compared with the original clone.

Cell culture and transfection. Prior to *in vivo* infection studies, we validated our expression vector system *in vitro* by transfecting human embryonic kidney (HEK) cells

and visualizing GFP and HA. HEK cells were the generous gift of Dr. Randy Blakely (Vanderbilt University). They were cultured as a monolayer in DMEM maintenance media (high glucose/l-glutamine) supplemented with 5% fetal bovine serum (Hyclone, Logan UT), 5% fetal calf serum (Hyclone), 0.5% penicillin/streptomycin. Cultures were maintained in 75 cm3 flasks at 37^{o}C in an atmosphere of humidified 95%O_2/5% CO_2. For the assays described below, cells were studied at 70-80% confluency.

Trypsinized cells were aliquotted to 6-well plates (Becton Dickinson, Franklin Lake NJ) 24 hr prior to transfection. Effectene Transfection Reagent (Qiagen) was used for the efficient transfection of the expression vector containing HA-*tub*/GFP (1 μg DNA/well). After three days' incubation, cells were harvested. Intact cells were visualized for GFP expression using an inverted fluorescence microscope (Nikon, TE 3000) and FITC filter. Additional cells were processed for Western blotting and detection of HA expression.

Immunoblotting. Cells were immunoprecipitated with 1 μl monoclonal anti-HA-peroxidase high affinity (3F10) antibody (Roche Molecular Biochemicals, Mannheim, Germany) overnight and incubated 2 hr with Protein A-Sepharose beads (Zymed Lab Inc., San Francisco CA). The precipitate was washed 3x with high salt wash buffer (20 mM HEPES, 0.3 M NaCl, 5 mM $MgCl_2$, 0.5% TritonX-100, pH 7.5) and 2x with low salt wash buffer (20 mM HEPES, 0.05 M NaCl, 5 mM $MgCl_2$, 0.5% TritonX-100, pH 7.5) (15). The washed precipitate was resuspended in 30 ml 2x Laemmli sample buffer (BioRad, Hercules CA) and incubated at room temperature, 20 min, for dissociation from the Sepharose beads. The mixture was centrifuged 5 min 16,000 x g, and the supernatant

was stored at –20°C for Western blotting. The sample was boiled at 100°C, resolved by 10% SDS-polyacrylamide gel electrophoresis (precast gel, Biorad), and transferred to a PVDF membrane (BioRad). After overnight blocking with BLOTTO (PBS, 0.01 M NaN_3, 0.05 % TWEEN 20, 5% nonfat dry milk, pH 7.3), membranes were washed 3x with wash buffer (PBS, 0.01 M NaN_3, 0.1% Tween 20, pH 7.3) and incubated with primary antibody (monoclonal HA-peroxidase, 1:500) for 60 min, 37°C, in diluent buffer (PBS, 0.01 M NaN_3, 0.1% Tween 20, 1% BSA, pH 7.3). Membranes were washed 3x with wash buffer, developed with ECL (Amersham), and exposed to film (Kodak).

Immunocytochemistry. Cannula placement and successful viral vector infection were verified in all rats following *in vivo* study. An observer blind to the experimental treatment groups evaluated cannula placement and GFP expression in each rat; only *in vivo* data from rats with adequate GFP expression in the ARC were included for analysis. Initial assays validated the neuronal co-expression of GFP and HA-*tub* proteins in HA-*tub*/GFP infected animals (Figure 2). This expression system has been shown to result in maximal gene expression at 3-5 days. We verified *in situ* GFP expression in the ARC over a time course of 3-6 days as further validation of the amplicon system prior to *in vivo* studies (data not shown). Rats were deeply anesthetized with pentobarbital (50 mg/ml; 2 ml/kg body weight) and perfused transcardially with 4% paraformaldehyde/PBS for immunocytochemistry as published and described previously (10) and immunocytochemistry was performed as previously described (8). Brains were removed, 40 μm vibratome (Leica, Nussloch, Germany) sections that included the entire hypothalamus (AP stereotaxic coordinates, -0.92 to –4.3 mm from bregma) were

prepared, and frozen for immunocytochemistry to localize HA and GFP expression. Free-floating sections were rinsed and permeabilized in PBS/0.01% sodium azide for 30 min at room temperature. Sections were blocked in PBS/0.01% sodium azide/0.025% Triton X-100/0.3% gelatin for 60 min at room temperature. Mouse monoclonal anti-HA (Babco, CA), diluted 1:1000 in blocking buffer, was added and sections were incubated overnight at 4^{o}C. Tissue sections were washed 3x, 10 min/wash, at room temperature in PBS/0.01% sodium azide/0.025% Triton X-100. Cy5 conjugated anti-mouse antibody (Kirkegaard & Perry Laboratories Inc., Gaithersburg MD), 1:500 in blocking buffer, was added for 45 min at room temperature. Sections were washed 3x, room temperature. They were mounted with a drop of Gel/Mount (Biomeda Corp.) and coverslipped for visualization with a Leica TCS SP Confocal Microscope system.

In vivo studies. Male albino rats (Simonsen Labs, Gilroy CA and Animal Technology Laboratories, Kent WA) were studied at the weight of 350-400 gm (see Table 1 for weights of rats at time of hypothalamic injection). All rats had *ad libitum* access to Purina rat chow and water throughout the studies. For the final experiments, rats had additional *ad libitum* access for 60 min/day five days/week to a high fat diet (Harlan Teklad [31]) for approximately five weeks. The diet was also available post-surgery and during the minipump infusion period. Both chow and high fat diet intake were quantitated. All rats received bilateral acute injections into the ARC, immediately followed by insertion of two Alzet osmotic minpumps (Alza, Palo Alto CA; 7-day minipumps with infusion rate approximately 0.5 ml/hr) subcutaneously into the intrascapular area. For this procedure, rats were previously implanted under ketamine/xylazine/0.9% saline (v/v/v=10/1.3/5.2) anesthesia with bilateral guide cannulas that terminated immediately dorsal to the ARC

(stereotaxic coordinates: AP –2.2. mm, DV –8.9 mm, ML +/- 0.4 mm). After complete recovery from guide cannula placement (documented as regain of pre-surgical body weight and a positive weight gain trajectory), rats were again anesthetized with isoflurane/oxygen (adjusted as needed). Viral particles (HA-*tub*-GFP or GFP-only) were injected via Hamilton syringe and microprocessor-controlled infusion pump (World Precision Instruments, SP 101i) at a rate of 2 μl over 10 min. The injector was left in place for 2 min. Immediately following the injection, minipumps were implanted and attached to the cannulas with vinyl tubing (Scientific Commodities Inc., Lake Havasu City AZ). Minipumps delivered either sterilized artificial CSF or a dose of insulin as indicated in the **RESULTS** section. Body weight, food intake, and water intake were measured for the subsequent six days. Animals were then euthanatized by anesthesia/perfusion as described above.

RESULTS

Validation of expression of the viral constructs. We evaluated the co-expression of HA-*tub* and GFP in infected HEK cells and in the medial hypothalamus. As shown in Figure 1, HEK cells infected with the HA-*tub*/GFP viral vector construct express both proteins. GFP fluorescence (Fig 1, left) was observed in whole cells; and HA was detected in a Western blot of an HA-immunoprecipitate of the infected HEK cells as compared with no detectable HA-immunoreactivity in the HEK cells that were non-infected and prepared simultaneously (Fig 1, right). Successful infection and co-expression of HA-*tub* and GFP in rat hypothalamus was established with fluorescence confocal microscopy, and one example is shown in Figure 2. We observed co-localization of HA and GFP in ARC neuronal processes (Figure 2a, HA immunofluorescence; Figure 2b, GFP fluorescence; Figure 2c, merged images). Because we observed co-expression of GFP and HA-*tub* in these initial controls, GFP expression was used subsequently for visual validation of the location of viral injection sites and the success of the infection in all experimental subjects. Figure 3a shows an injection track for the (bilateral) injection dorsal to the medial ARC, and Figure 3b shows at higher magnification, GFP expression in individual cells in the ARC. Although we were not able to identify the phenotype of infected neurons in this study, the abundant expression of insulin receptors in the ARC makes it reasonably likely that at least a portion of insulin receptor-expressing neurons were successfully infected.

We evaluated the effect of intra-ARC control injection/infusion treatments on body weight and food intake over the subsequent 6 days post-minipump implant. Control

(GFP) viral infection had a modest but significant effect to suppress body weight independent of insulin treatment in comparison to rats that received either sucrose (the viral particle vehicle) or CSF injection: Average weight change over the six minipump days was GFP/CSF= -13±3 gm (n=12); CSF/CSF= 0.2±2 gm (n=10); sucrose/CSF= 3±3 gm (n=5) (comparisons: GFP/CSF vs. CSF/CSF, p=0.004; GFP/CSF vs. Suc/CSF, p=0.012). GFP vector expression likewise had a modest but significant effect to suppress food intake in the GFP/CSF vs. CSF/CSF groups (p=.015). Thus, all studies with intra-ARC insulin infusions included GFP-vector injections as controls.

Lack of effect of exogenous *tub* expression on insulin-induced catabolic effects in chow-fed rats. ARC infusion of insulin resulted in a dose-related weight loss in rats infected with either GFP or HA-*tub* vector (Figure 4). All rats received vector injections followed by infusion of artificial CSF; 10 mU/day insulin; or 20 mU/day insulin directly into the medial ARC. In the GFP-injected rats (solid lines), there was a significant overall dose effect for insulin infusion into the ARC to decrease body weight ($F_{2,18}$ =6.448, p=.005); a significant dose by time interaction ($F_{1,204}$ =2.545, p=.007); and significance across days for individual insulin doses to decrease body weight (CSF vs. 10 mU insulin/day, p=.001; CSF vs. 20 mU insulin/day, p<.0001; 10 vs. 20 mU insulin/day, p<.0001). Figure 4 also shows the corresponding dose response curve for rats receiving HA-*tub* injections (dashed lines) followed by CSF, or 10 or 20 mU/day insulin infusion into the ARC. There was no overall or interactive effect of *tub* treatment with days, insulin treatment, or day x insulin combination as compared to GFP control animals. Thus, exogenous expression of

tub in the ARC had no effect on either baseline body weight, or the efficacy of insulin to decrease body weight, in normal weight rats maintained on a diet of normal rat chow.

Insulin infusion into the ARC significantly decreased food intake. Although intake was comparably suppressed during the first 24 hr post-injection/implant ("Day 1") among the groups, there was a significant overall dose-effect for insulin to decrease food intake during Days 2-6 ($F_{2,62}$ =3.828; p=.027). Both doses of insulin were significantly effective in decreasing food intake, as evaluated by post-hoc unpaired t-test (520$\pm$12 vs. 488$\pm$8 kcal, 0 vs. 10 mU insulin, p= .038; 520$\pm$12 vs. 464$\pm$20 kcal, 0 vs. 20 mU insulin, p=.021). HA-*tub* expression had no effect on cumulative chow consumption at any dose of insulin (Figure 5; GFP vs. *tub* comparisons). There was no effect of either insulin or *tub* or an interactive effect of the two, on cumulative water intake over the six days post-minipump implant.

The efficacy of insulin to decrease body weight is impaired with high fat diet feeding and is further impaired by exogenous *tub* expression. Because previous studies have shown that the efficacy of insulin to decrease body weight is impaired in rats given access to a high fat diet (HFD) even in the absence of significant diet-induced body weight gain (2,6), we hypothesized that *tub*—although not effective in enhancing insulin action in chow-fed rats--might act to enhance or restore sensitivity to insulin in the ARC of rats fed a high fat diet. We gave rats access to HFD for 60 min/day, five days/week for approximately five weeks prior to surgery. All rats also had *ad libitum* access to rat chow. Rats were then tested with intra-ARC injections of GFP or HA-*tub*/GFP vector and

infusions of 20 mU insulin/day. As shown in Figure 6, rats given access to HFD had a significantly attenuated body weight decrease in response to 20 mU/day insulin relative to the chow-fed cohort, confirming that HFD makes rats resistant to insulin action in the ARC. There was a significant overall effect of the HFD ($F_{1,18}$ = 6.679, p=0.02) and the effect was significant for individual days 1 through 5 (p= 0.03, 0.04, 0.002, 0.02, and 0.02 for the respective five days). The average change of body weight between the chow- and HFD-fed rats across the infusion period was likewise significant (chow, -32+1 gm; HFD, -21+2 gm, p<.0001).

In contrast to its lack of effect on insulin action in chow-fed rats, and in contrast to our predicted effect of *tub* in HFD-fed rats, HA-*tub* expression in the ARC further blunted the effect of insulin to decrease body weight in these animals (Figure 7). Average within-subjects' body weight decrease across the six days post-implant was significantly greater in the 'GFP' vs. the *tub* rats (-21$\pm$3 gm vs. –14$\pm$4 gm, p=0.03). There was a significant day x treatment interaction ($F_{2,18}$=2.621, p=0.02), and significant individual differences on days 3 through 6 (p= 0.05, 0.03, 0.04, and 0.02 for each day respectively). Average caloric intake for five days prior to minipump implant was comparable for GFP vs. *tub* rats (103$\pm$2 vs. 106$\pm$2 kcal/day, respectively). Total caloric intake across the six days of insulin infusion was lower in the GFP vs. HA-*tub*/GFP groups (438$\pm$28 vs. 507$\pm$19 kcal, p=0.05); this change was a composite of decreases in both HFD intake (159$\pm$13 vs. 181$\pm$17 kcal, p= 0.33) and chow intake (279$\pm$32 vs. 326$\pm$29 kcal, p= 0.31). To validate that this effect of HA-*tub* was not merely an additive effect of the 20 mU/day insulin treatment with an independent effect of *tub* on its own to increase body weight in rats

having access to HFD, we studied a series of rats maintained on the HFD, injected with GFP or HA-*tub*-GFP vector, but infused with CSF. Comparable to what we observed in the '0 mU insulin' chow-fed rats, there was no difference in body weight across the six days of infusion between GFP and *tub* rats. That is, exogenous *tub* expression by itself did not cause weight gain in CSF-infused HFD rats (data not shown). Therefore it appears that exogenous expression of *tub* in rat ARC, in association with HFD availability, further reduces insulin action.

DISCUSSION

In this study we demonstrated that insulin infusion into the rat ARC has catabolic effects to decrease body weight and food intake, and this effect is blunted in rats fed a high fat snack in addition to rat chow, thus demonstrating behavioral insulin resistance at the level of the hypothalamus. Additionally, exogenous expression of *tub* does not result in enhanced efficacy of insulin to decrease food intake and body weight. In rats maintained on normal rat chow, *tub* did not enhance the action of endogenous insulin (as demonstrated by its ineffectiveness in rats infused with artificial CSF), nor the action of exogenous insulin (10 or 20 mU/day) as compared to insulin effects in GFP-expressing animals. Further, in contrast to our originally hypothesized outcome, *tub* overexpression did not reverse the impairment of insulin's catabolic actions in rats given access to HFD: 20 mU insulin/day was less effective in HFD-fed rats, comparable to what has been previously reported (2,6), and this impairment was not rescued by exogenous *tub* expression. To the contrary, exogenous *tub* expression in HFD-fed rats further impaired the catabolic action of insulin, and this last observation also suggests that the lack of effect of *tub* in chow-fed rats was not due to lack of expression within insulin-sensitive neurons, as a clear interaction was observed when exogenous insulin infusion was combined with *tub* infection in the HFD-fed rats.

Our study represents the first *in vivo* exploration of *tub* function in energy balance regulation of normal rats. Although we did not quantify 'tub' protein per se in our rats, increased expression of target proteins has been observed by ourselves (8) and other labs using this HSV amplicon system. Our *in vitro* and immunocytochemistry controls

validated the co-expression of GFP and HA-tub, thus it seems reasonable to conclude that we were successful in expressing or over-expressing rat 'tub' in the ARC. One speculation from our findings is that expression of *tub* beyond normal endogenous amounts may not enhance insulin signaling—as represented by its actions to decrease food intake and body weight—and in fact excess amounts of *tub* may impair insulin action. *In vitro* biochemical studies have suggested the possibility that *tub* may act as an adaptor for insulin signaling (15). However, *tub* function is still poorly understood both *in vivo* and *in vitro*, thus one can only speculate on mechanisms whereby this might occur. For example, one might speculate that an intracellular overabundance of *tub* might lead to it serving as an adaptor molecule for signaling pathways that are antagonistic to insulin. Another possibility would be that intracellular distribution of *tub* in the nucleus vs. cytoplasm might be altered with its overexpression. Shapiro and colleagues have provided evidence that *tub* release from the plasma membrane occurs in association with activation of $G\alpha_q$-coupled receptors (26), and they speculate that this release leads to nuclear translocation of *tub*. One might then hypothesize that enhanced concentrations of *tub* would be released in association with stimulation of $G\alpha_q$-coupled receptors in the ARC by endogenous ligands whose action opposes the catabolic effects of insulin, for example melanin-concentrating hormone (MCH). Receptors for MCH are expressed in the ARC (25). Such an effect may have synergized with the relative insulin resistance in the ARC that occurred in the HFD-fed rats. Finally, the impaired insulin action in HFD-fed rats (as reflected in blunted body weight loss) may result in impairment in the tyrosine phosphorylation of *tub*. Overexpression of *tub* might result in an imbalance of phosphorylated (insulin-enhancing) vs. non-phosphorylated (nuclear translocating) forms

and have a net effect to antagonize insulin action further. These are speculative possibilities but lend themselves to direct testing in cellular *in vitro* systems.

In conclusion, loss of *tub* function developmentally results in a mild adult-onset obesity. Overexpression of *tub* in the mature rat hypothalamus does not yield an opposite phenotype, i.e., a tendency to eat less than normal and to lose weight, but it appears to have a fairly acute effect to impair the catabolic effect of insulin. These findings suggest that the *in vivo* action(s) of *tub* are, not surprisingly, more complex than those observed in highly defined cellular systems. Future *in vivo* studies targeting other specific hypothalamic nuclei, or testing the efficacy of specific $G\alpha_q$-coupled receptor-activating ligands in the hypothalamus, should lead to a more complete understanding of the role of *tub* protein in the normal regulation of food intake and body weight. Finally our study highlights again the influence of diet composition on insulin action in the CNS. Although virtually nothing is known about the regulation of *tub* synthesis in normal animals (to date, one report describes effects of a hypothyroid state to increase, decrease, or not change *tub* expression in the rat brain, with region-specific effects and little effect on the medial hypothalamus [17]), one might speculate that a propensity for elevated endogenous levels of *tub* might predispose some populations of individuals to become resistant to adiposity signals such as insulin when combined with dietary exposure to moderate or high fat, making these individuals more vulnerable to diet-induced weight gain.

PERSPECTIVES

Downstream intracellular signaling pathways for insulin in the medial hypothalamus may represent novel targets for therapeutic strategies in the treatment of obesity. To this end, the function, regulation, and potential pathophysiologic alterations of key signaling molecules need to be understood at both the cellular and the behavioral levels. In addition to providing specific new insight into the action of one candidate signaling molecule, ‘tub’, the current study emphasizes the need for experimental approaches that go beyond knockout mouse technology and cultured cell systems, in order to fully elucidate the function of signaling molecules in circumstances that reflect the human obesity environment.

ACKNOWLEDGEMENTS

These studies were funded by an Innovation Award from the American Diabetes Association. Dianne Figlewicz Lattemann is supported by the Dept. of Veterans Affairs and NIH Grant DK RO1-40963. John F. Neumaier is supported by NIH Grant MH 63303. We thank Drs. Scott Ng-Evans and Al Sipols for helpful discussions, and Marcy Hoen for technical assistance with the histological evaluations. We thank Amber Caracol for assistance in the initial characterization of the HA-tub vector.

REFERENCES

1. Ahima RS, Saper CB, Flier JS, and Elmquist JK. Leptin regulation of neuroendocrine systems. *Front Neuroendocrinol* 21: 263-307, 2000.

2. Arase K, Fisler JS, York DA, and Bray GA. Intracerebroventricular infusions of 3-OHB and insulin in a rat model of dietary obesity. *Am J Physiology* 255: R974-R981, 1988.

3. Baskin DG, Figlewicz Lattemann D, Seeley RJ, Woods SC, Porte D Jr., and Schwartz MW. Insulin and leptin: dual adiposity signals to the brain for the regulation of food intake and body weight. *Brain Research* 848: 114-123, 1999.

4. Boggon TJ, Shan W-S, Santagata S, Myers SC, and Shapiro L. Implication of tubby proteins as transcription factors by structure-based functional analysis. *Science* 286: 2119-2125, 1999.

5. Bolanos CA, Perrotti LI, Edwards S, Eisch AJ, Barrot M, Olson VG, Russell DS, Neve RL, and Nestler EJ. Phospholipase cγ in distinct regions of the ventral tegmental area differentially modulates mood-related behaviors. *J Neurosci* 23: 7569-7576, 2003.

6. Chavez M, Riedy CA, VanDijk G, and Woods SC. Central insulin and macronutrient intake in the rat. *Am J Physiology* 271: R727-R731, 1996.

7. Chung WK, Goldberg-Berman J, Power-Kehoe L, and Leibel RL. Molecular mapping of the tubby (tub) mutation on mouse chromosome 7. *Genomics* 32: 210-217, 1996.

8. Clark MS, Sexton TJ, McClain M, Root D, Kohen R, and Neumaier JF. Overexpression of 5-HT1B receptor in dorsal raphe nucleus using Herpes Simplex Virus gene transfer increases anxiety behavior after inescapable stress. *J Neuroscience* 22: 4550-4562, 2002.

9. Coleman DL. Fat (fat) and Tubby (tub): two autosomal recessive mutations causing obesity syndromes in the mouse. *J Heredity* 81: 424-427, 1990.

10. Evans SB, Wilkinson CW, Bentson K, Gronbeck P, Zavosh A, and Figlewicz DP. PVN activation is suppressed by repeated hypoglycemia but not antecedent corticosterone in the rat. *Am J Physiology* 281: R1426-R1436, 2001.

11. Figlewicz DP. Adiposity signals and food reward: expanding the CNS roles of insulin and leptin. *Am J Physiology* 284: R882-R892, 2003.

12. Guan X-M, Yu H, and Van der Ploeg LHT. Evidence of altered hypothalamic pro-opiomelanocortin/neuropeptide Y mRNA expression in tubby mice. *Mol Brain Res* 59: 273-279, 1998.

13. Heikenwalder MF, Koritschoner NP, Pajer P, Chaboissier MC, Kurz SM, Briegel KJ, Bartunek P, and Zenke M. Molecular cloning, expression and regulation of the avian tubby-like protein 1 (tulp1) gene. *Gene* 273: 131-139, 2001.

14. Ikeda A, Nishina PM, and Naggert JK. The tubby-like proteins, a family with roles in neuronal development and function. *J Cell Science* 115: 9-14, 2002.

15. Kapeller R, Moriarty A, Strauss A, Stubdal H, Theriault K, Siebert E, Chickering T, Morgenstern JP, Tartaglia LA, and Lillie J. Tyrosine phosphorylation of Tub and its association with Src Homology 2 domain-containing proteins implicate Tub in intracellular signaling by insulin. *J Biol Chem*274: 24980 -24986, 1999.

16. Kleyn PW, Fan W, and Kovats SG. Identification and characterization of the mouse gene tubby: a member of a novel gene family. *Cell* 85: 281-290, 1996.

17. Koritschoner NP, Alvarez-Dolado M, Kurz SM, Heikenwalder MF, Hacker C, Vogel F, Munoz A, and Zenke M. Thyroid hormone regulates the obesity gene tub. *EMBO Reports* 21: 499-504, 2001.

18. Li QZ, Wang CY, Shi JD, Ruan QG, Eckenrode S, Davoodi-Semiromi A, Kukar T, Gu Y, Lian W, Wu D, and She JX. Molecular cloning and characterization of the mouse and human TUSP gene, a novel member of the tubby superfamily. *Gene*273: 275 - 284, 2001.

19. Neve RL, Howe JR, Hong S, and Kalb RG. Introduction of the glutamate receptor subunit 1 into motor neurons in vitro and in vivo using a recombinant herpes simplex virus. *Neuroscience* 79: 435-447, 1997.

20. Noben-Trauth K, Naggert JK, North MA, and Nishina PM. A candidate gene for the mouse mutation tubby. *Nature* 380: 534-538, 1996.

21. North MA, Naggert JK, Yan Y, Noben-Trauth K, and Nishina PM. Molecular characterization of TUB, TULP1, and TULP2, members of the novel tubby gene family and their possible relation to ocular diseases. *Proc Natl Acad Sci* 94: 3128-3133, 1997.

22. Obici S, Feng Z, Karkanias G, Baskin DG, and Rossetti L:.Decreasing hypothalamic insulin receptors causes hyperphagia and insulin resistance in rats. *Nature Neuroscience* 5: 566-572, 2002.

23. Ohman M, Oksanen L, Kainulainen K, Janne OA, Kaprio J, Koskenwo M, Mustajoki P, Kontula K, and Peltonen L. Testing of human homologues of murine obesity genes as candidate regions in Finnish obese sib pairs. *Eur J Human Genetics* 7: 117-124, 1999.

24. Sahly I, Gogat K, Kobetz A, Marchant D, Menasche M, Castel M-N, Revah F, Dufier J-L, Guerre-Millo M, and Abitbol MM. Prominent neuronal-specific tub gene expression in cellular targets of tubby mice mutation. *Human Mol Genetics* 7: 1437-1447, 1998.

25. Saito Y, Cheng M, Leslie FM, and Civelli O. Expression of the melanin-concentrating hormone (MCH) receptor mRNA in the rat brain. *J Comp Neurology* 435: 26-40, 2001.

26. Santagata S, Boggon TJ, Baird CL, Gomez CA, Zhao J, Shan WS, Myszka DG, and Shapiro L. G-protein signaling through tubby proteins. *Science* 292: 2041-2050, 2001.

27. Schwartz MW, Woods SC, Porte D Jr., Seeley RJ, and Baskin DG. Central nervous system control of food intake. *Nature* 404: 661-671, 2000.

28. Stubdal H, Lynch CA, Moriarty A, Fang Q, Chickering T, Deeds JD, Fairchild-Huntress V, Charlat O, Dunmore JH, Kleyn P, Huszar D, and Kapeller R. Targeted deletion of the tub mouse obesity gene reveals that tubby is a loss-of-function mutation. *Mol Cell Biol* 20: 878-882, 2000.

29. Tecott LH, Sun LM, Akana SF, Strack AM, Lowenstein DH, Dallman MF, and Julius D. Eating disorder and epilepsy in mice lacking 5HT2c serotonin receptors. *Nature* 374: 542-546, 1995.

30. VanDijk G, de Groote C, Chavez M, van der Werf Y, Steffens AB, and Strubbe JH. Insulin in the arcuate nucleus of the hypothalamus reduces fat consumption in rats. *Brain Research* 777: 147-152, 1997.

31. Zhang M and Kelley AE. Enhanced intake of high-fat food following striatal mu-opioid stimulation: microinjection mapping and Fos expression. *Neuroscience* 99: 267-277, 2000.

32. Zhang Y, Proenca R, Maffei M, Barone M, Leopold L, and Friedman JM. Positional cloning of the mouse obese gene and its human homologue. *Nature* 372: 425-432, 1994.

FIGURE LEGENDS

Figure 1. Expression of the HA-*tub*-GFP construct in infected HEK cells. **(a)** GFP fluorescence expression in intact cells. **(b)** Western blot of HA-immunoprecipitate blotted for HA-immunoreactivity. No HA-immunoreactivity is observed in HEK cells infected with the control construct (GFP-only).

Figure 2. Expression of the HA-*tub*-GFP construct *in vivo* in arcuate nucleus neurons visualized by confocal microscopy. **(a)** HA immunofluorescence; **(b)** GFP fluorescence; **(c)** merged images showing co-localization of HA and GFP.

Figure 3. Cannula placement and regional expression of the HA-*tub*-GFP construct: visual *post hoc* criterion for successful infection. **(a)** example of bilateral cannula placement immediately dorsal to the arcuate nucleus; **(b)** GFP expression is abundant and predominantly within the arcuate nucleus.

Figure 4. Lack of effect of *tub* overexpression on the action of insulin to decrease body weight in chow-fed rats. Data are within-subjects' change of body weight in gm, relative to body weight on the day of minipump implant. Key: Triangles, CSF infusion; diamonds, 10 mU/day insulin; circles, 20 mU/day insulin; solid lines and filled symbols, GFP injection; dashed line and open symbols, HA-*tub* injection. GFP/CSF, n = 12; *tub*/CSF, n = 8; GFP/10 mU/day insulin, n = 11; *tub*/10 mU/day insulin, n = 15; GFP/20 mU/day insulin, n = 8; *tub*/20 mU/day insulin, n=11. See text for statistical analyses.

Figure 5. Lack of effect of *tub* overexpression on food intake in chow-fed rats. Data correspond to the rats whose body weight data are shown in Figure 4.

Figure 6. The effectiveness of insulin to decrease body weight is impaired in rats given access to high fat diet (HFD, 60 min/day; 5 days/wk). All rats received 20 mU/day insulin following five-weeks' access to high fat diet in addition to *ad libitum* rat chow. Data are within-subjects' change of body weight in gm, relative to body weight on the day of minipump implant. * $p<.05$ between groups, unpaired t-test, at individual days. See Results for additional statistical analysis.

Figure 7. *Tub* overexpression in the arcuate nucleus impairs the effectiveness of insulin to decrease body weight in rats given access to high fat diet (HFD). All rats were infused with 20 mU insulin/day following injection of GFP vector (identical group to that shown in Figure 6) or HA-*tub* vector. Data are within-subjects' change of body weight in gm, relative to body weight on the day of minipump implant. * represents significant difference ($p<0.05$) between groups at the individual days, unpaired t-test.

Table 1. Weights for Experimental Groups at Time of Minipump Implant

		Body Weight, gm
I.	**CHOW ONLY**	
	CSF--GFP (n=12)	377±5
	CSF--*tub* (n=9)	375±3
	Insulin 10 mU/day—GFP (n=11)	388±3
	Insulin 10 mU/day—*tub* (n=16)	374±3
	Insulin 20 mU/day—GFP (n=8)	391±6
	Insulin 20 mU/day—*tub* (n=11)	399±5
II.	**CHOW + HFD**	
	Insulin 20 mU/day—GFP (n=12)	402±6
	Insulin 20 mU/day—*tub* (n=12)	397±6
	CSF—GFP (n=4)	420±14
	CSF—*tub* (n=4)	410±5
III.	**CONTROLS**	
	Chow-fed CSF—sucrose (n=5)	374±13
	Chow-fed CSF—CSF (n=10)	406±3

GFP fluorescence & HA Western blot

A

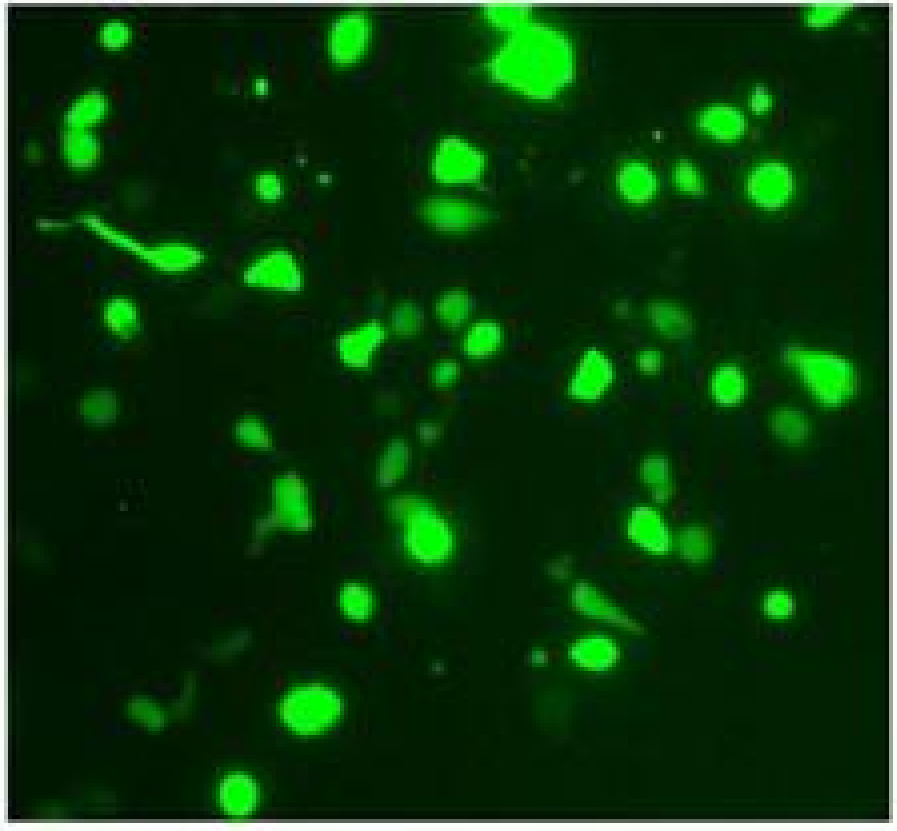

B

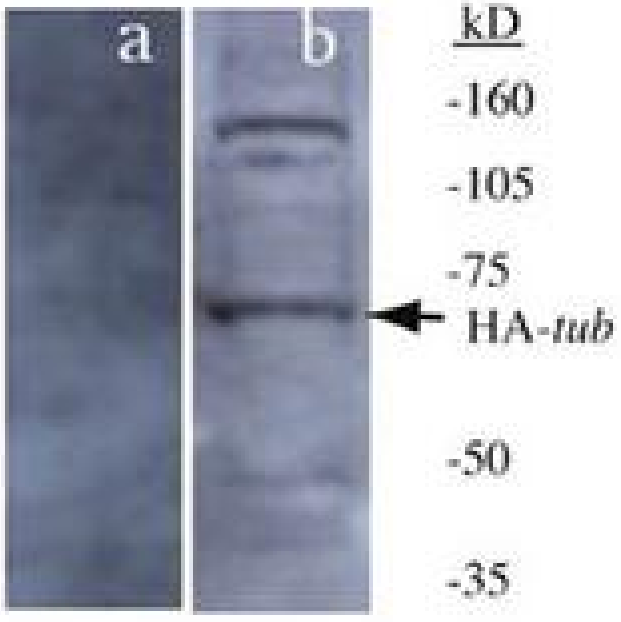

a: wild-type cells
b: HA-*tub*-GFP virus infected cells

Co-localization of GFP and HA-*tub*

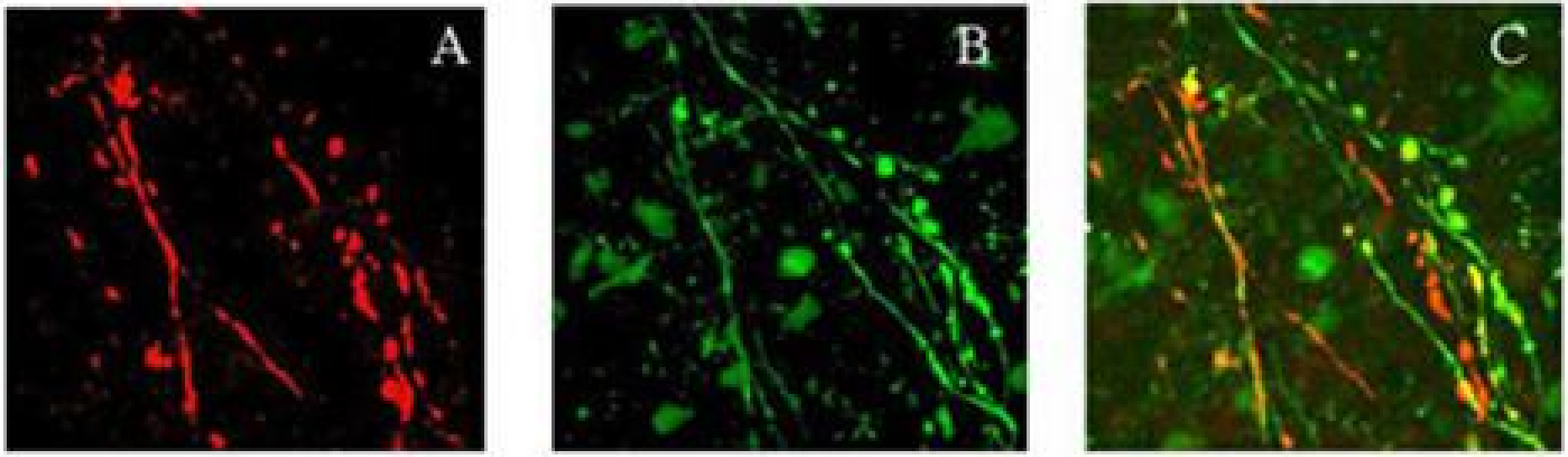

E-00427-2003.R1 Fig 2

Cannula Placement and GFP Expression in Arcuate Nucleus of Rat Brain

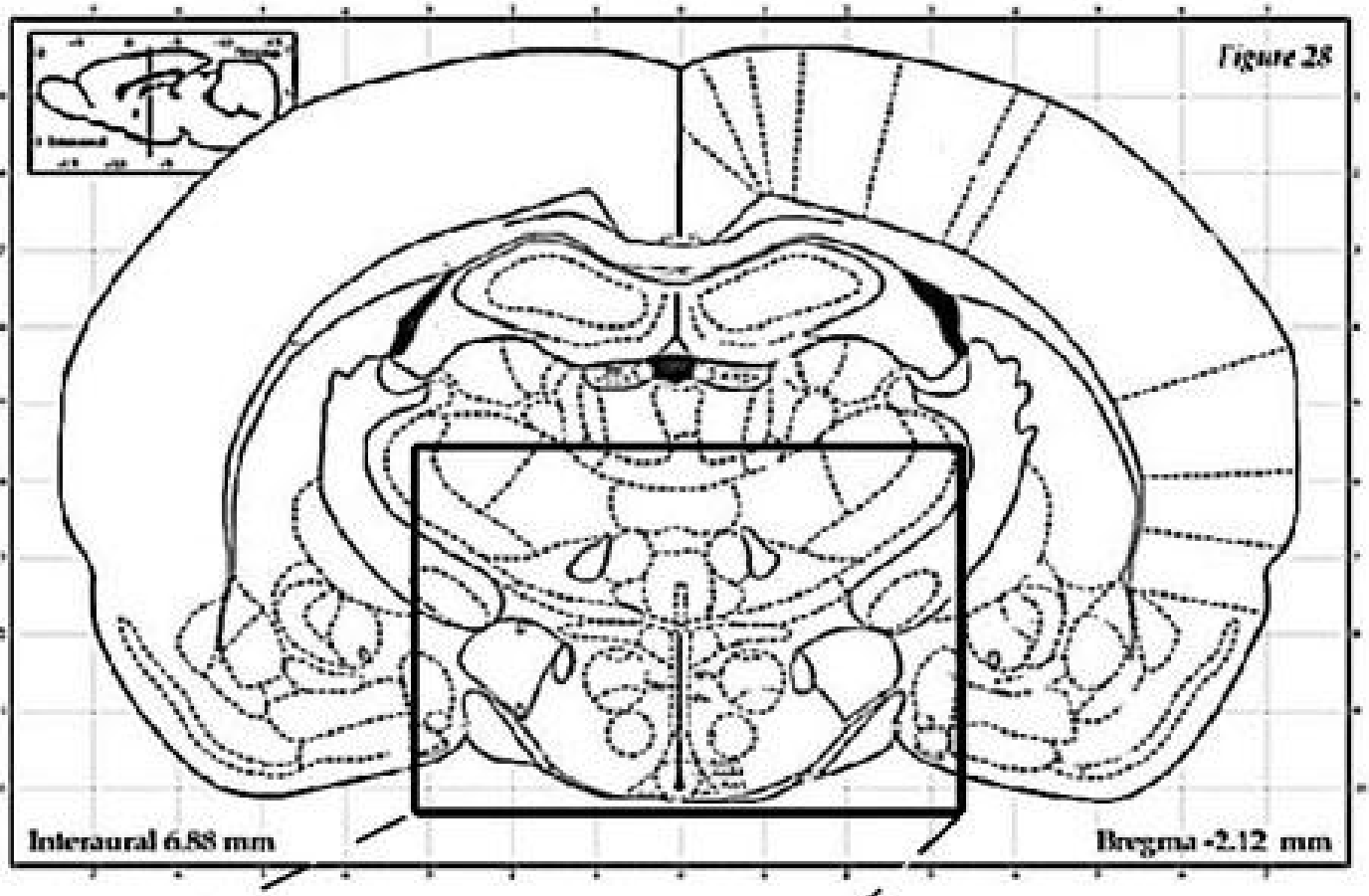

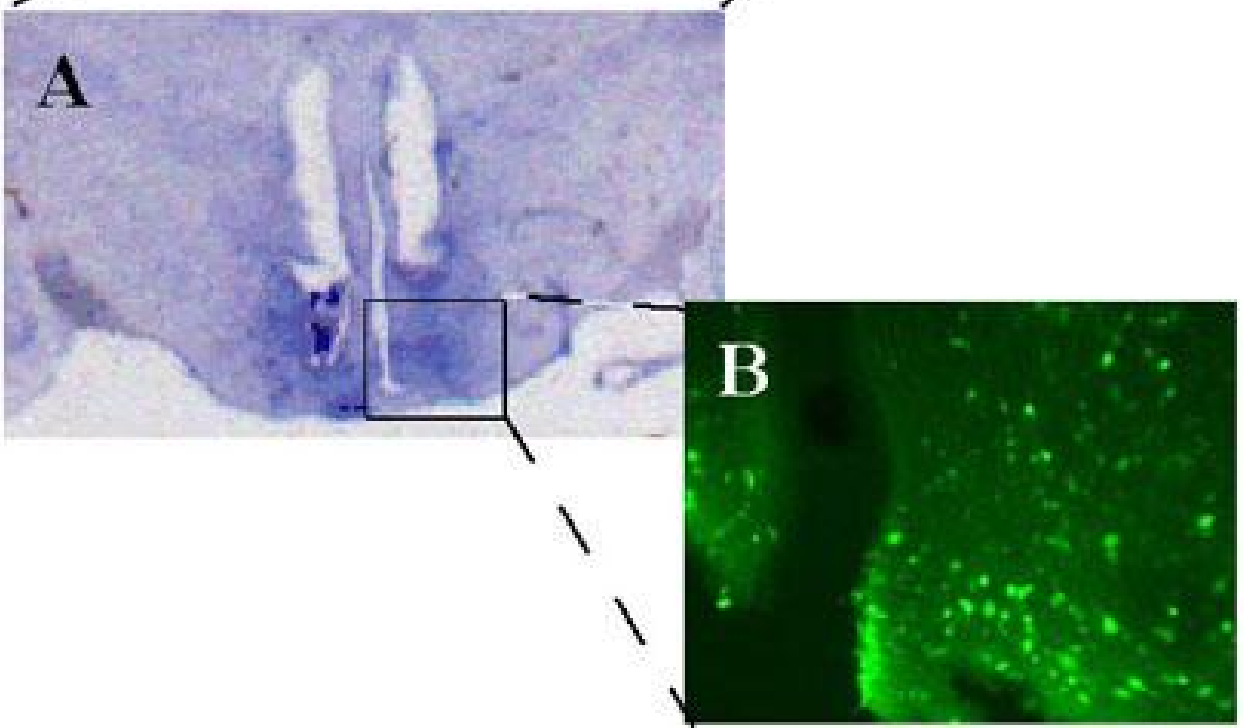

Effect of GFP, Tub and Insulin in the Arcuate Nucleus on Body Weight

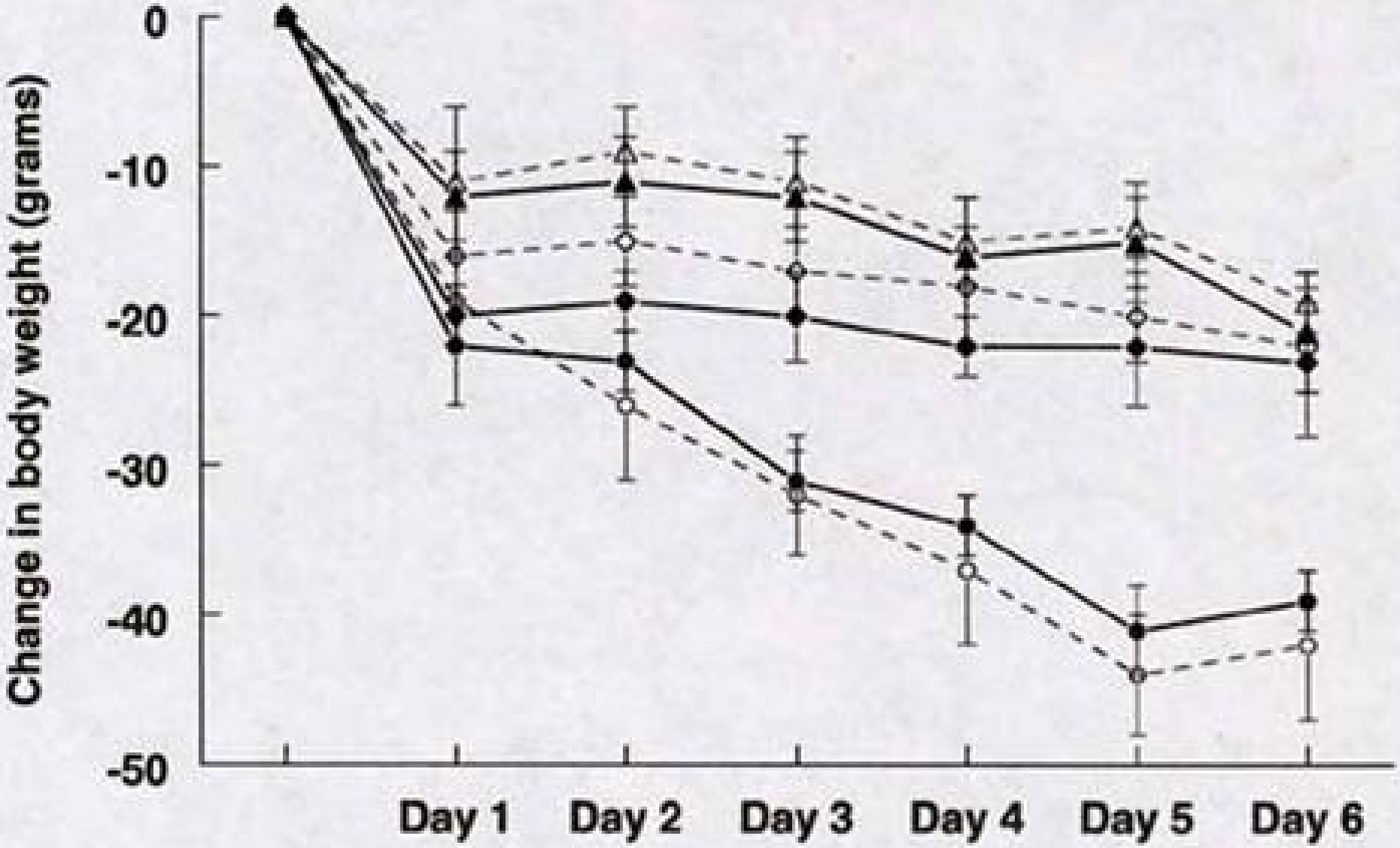

Effect of ARC Insulin Infusion on Days 2-6 Food Intake in Chow-fed Rats

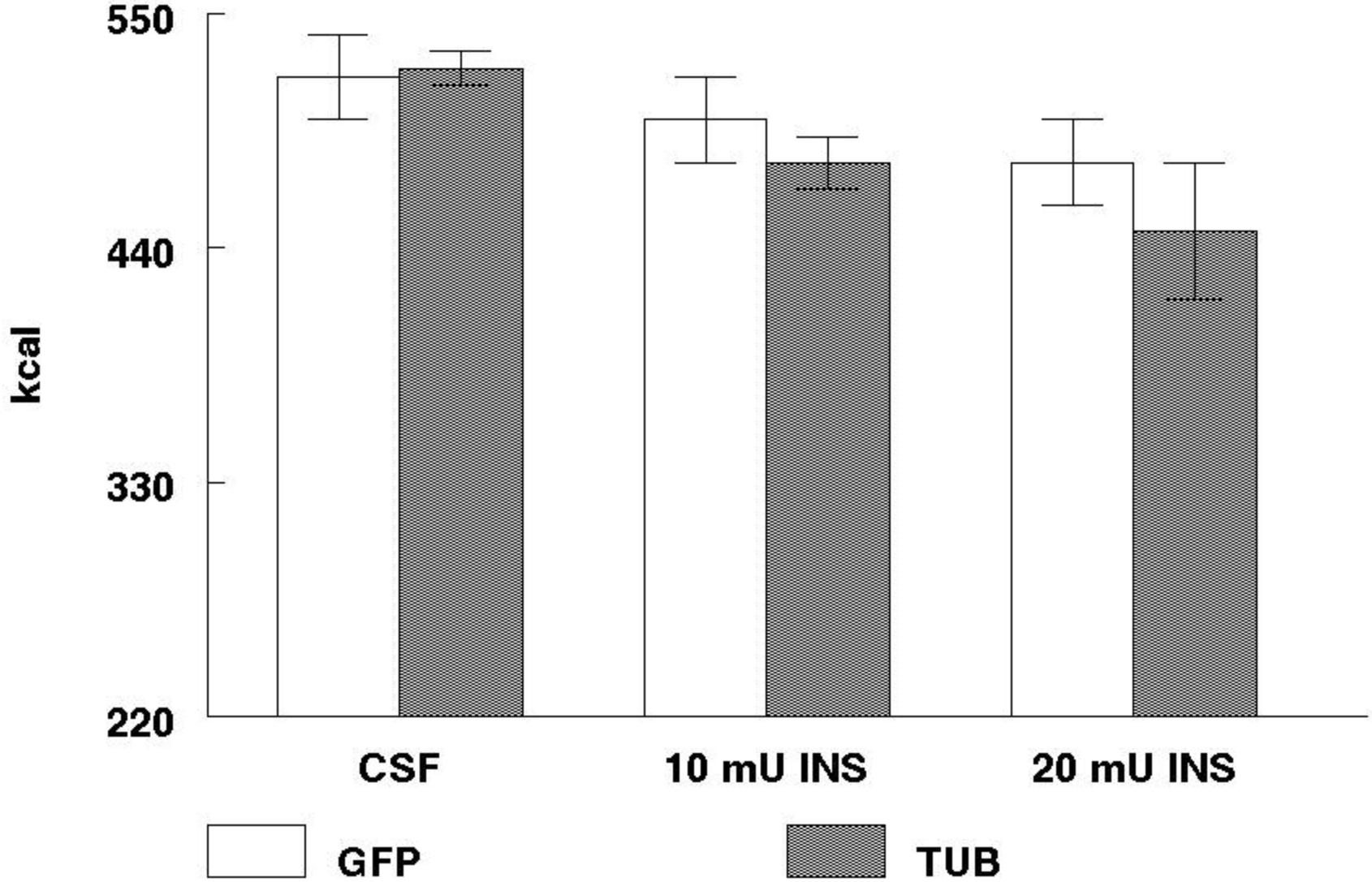

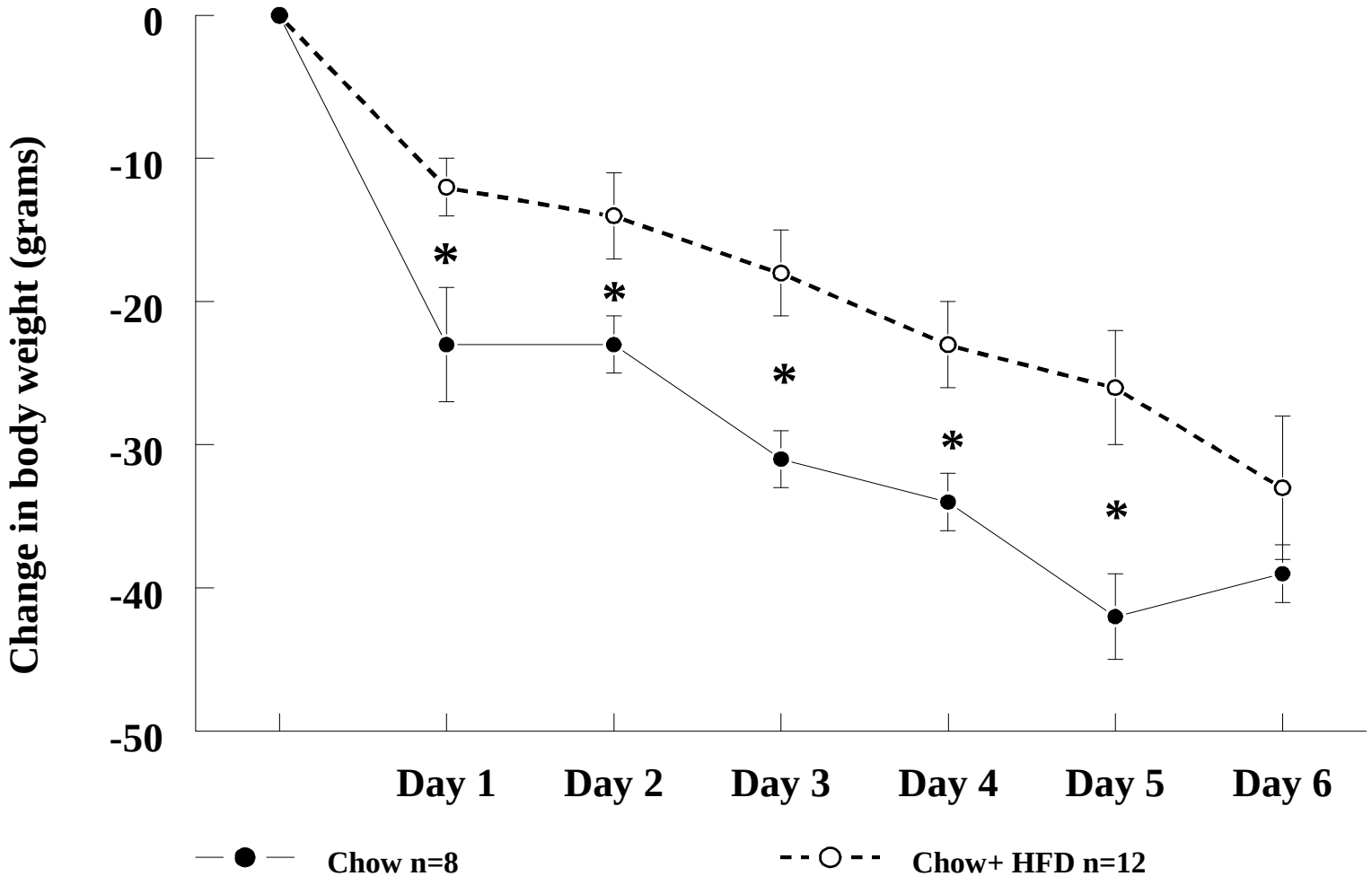
0
-10
-20
-30
-40
-50
Change in body weight (grams)
*
*
*
*
*
Day 1
Day 2
Day 3
Day 4
Day 5
Day 6
Chow n=8
Chow+ HFD n=12

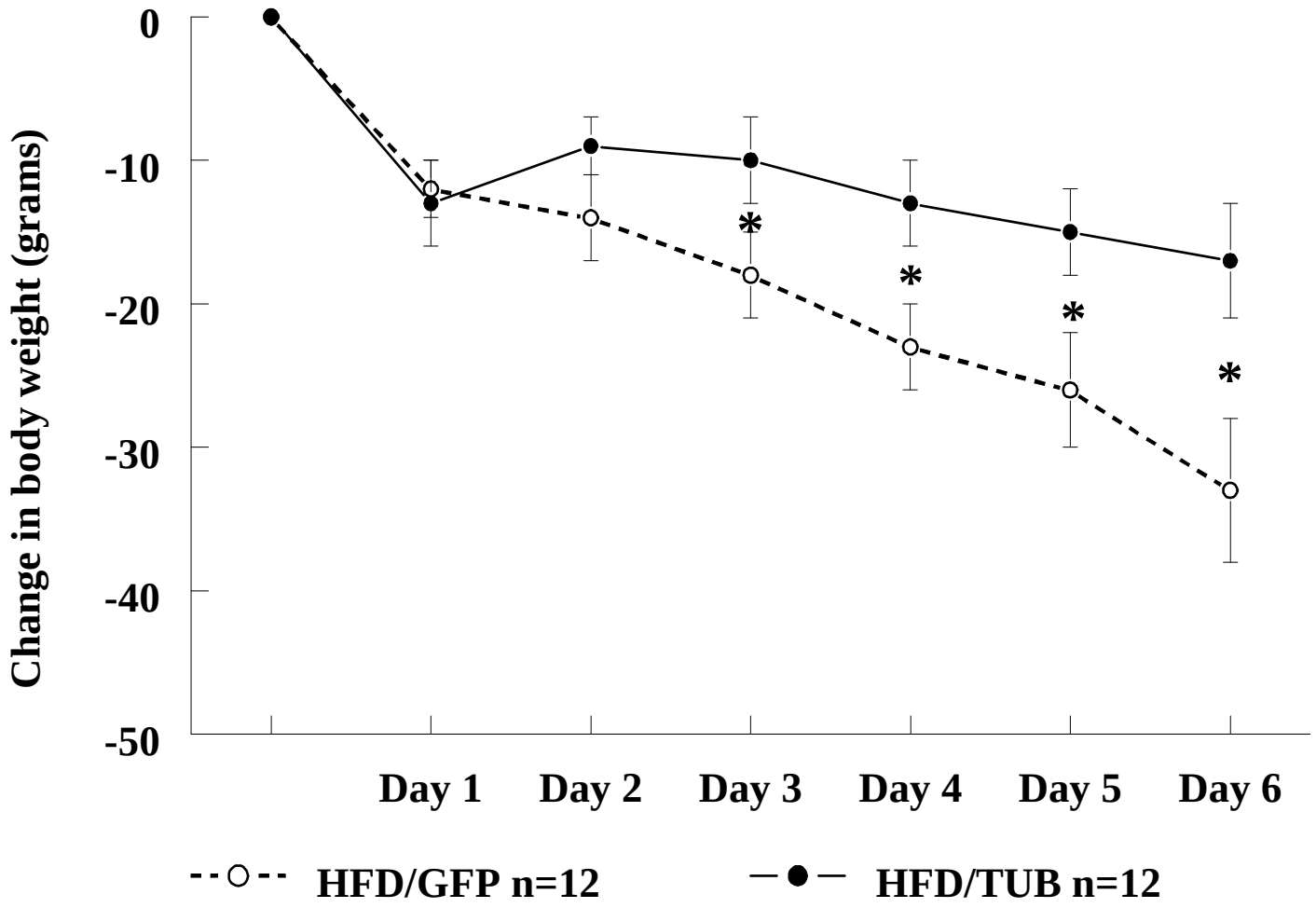
0
-10
-20
-30
-40
-50
Change in body weight (grams)
Day 1
Day 2
Day 3
Day 4
Day 5
Day 6
*
*
*
*
HFD/GFP n=12
HFD/TUB n=12